IOSR Journal of Environmental Science, Toxicology and Food Technology (IOSR-JESTFT)
e-ISSN: 2319-2402,p- ISSN: 2319-2399.Volume 13, Issue 9 Ser. I (September. 2019), PP 11-17
www.iosrjournals.org

Nondestructive Determination of Rice (with Chaff) Protein Content by Using Hyperspectral Imaging Technique

Zhehao Zhang[1], Zhishang Ren[1], Shuhua Wu[1], Juan Du[1], Xiang Yin[1],Chengqian Jin[1,3], Chengye Ma[1,2*]

[1]*School of Agricultural Engineering and Food Science, Shandong University of Technology, Zibo 255000, China;*
[2]*Key Laboratory of Shandong Provincial Universities for Technologies in Functional Agricultural Products, Zibo 255000, China;*
[3]*Nanjing Research Institute for Agricultural Mechanization of Ministry of Agriculture and Rural Affairs, Nanjing 210014, China*
Corresponding Author: Zhehao Zhang

Abstract*: Protein content is a basic and important quality indicator for rice and important for its overall quality during harvesting. Hyperspectral imaging technology(HSI)which is a fast and nondestructive detection technology was used to evaluate the rice (with chaff)protein content and quality. Partial least squares regression(PLSR) was used to build a calibration model (calibration coefficient= 0.992, root mean square error of calibration = 0.697%), across-validation model (cross-validation coefficient= 0.993, root mean square error of cross-validation = 0.624%) and a predictive model (prediction coefficient= 0.970, root mean square error of prediction = 1.03%). The characteristic wavelengths in a full wavelength range were selected to establish multiple characteristic wavelength calibration models and cross-validation models. The characteristic wavelength model can reduce scanning error and improve scanning efficiency. The model of the four characteristic wavelengths was selected as the optimal experimental model. The establishment of the full and characteristic wavelength models showed that HSI can detect the rice grain protein contentexcellently.*

Keywords: *Hyperspectral imaging, Rice, Protein content, Partial least squares regression, Characteristic wavelength selection*

Date of Submission: 28-08-2019 Date of Acceptance: 12-09-2019

I. Introduction

Rice is consumed as a staple food by over one-half of the world's population and accounts for approximately 95% of Asian food production (Maraseni et al., 2018, Sompong R et al., 2011).Rice possesses a considerable amount of starch, protein, fat and some nutrients (Lin et al., 2015, Naito et al., 2015).In China, rice is planted in a large area that accounts for a quarter of China's total food crops. However, with the growth of the world population and the continuous improvement of people's living and medical standards, people's requirements for food quality continuously increase. The demand for the nutritional quality of rice is also high. The quality and taste after cooking of rice are mainly determined by nutrient content and type. Protein is one of the most important nutrient components in rice, and its content directly determines the quality of rice nutrients. The protein quality in rice is superior to that in wheat, and the kinds of protein in rice vary. Rice is rich in glutelin(70.8%), but large amounts of albumin(12.5%) and globulin(13.9%) are present as well (Wattanasiritham et al., 2016); the amino acid composition of rice is also good. Therefore, the rapid detection of rice protein content is extremely important. A strict set of testing standards is required in detecting rice protein content. Conventional methods, such as Kjeldahl, biuret-fixed nitrogen method, ultraviolet absorption-fixed nitrogen method and phenol reagent methods, can also detect the protein content of rice; however, the operation process is complicated and destructive (Kamruzzaman et al., 2015, Jackson et al., 1991, Zhang et al., 2017). This process also consumes requires manpower and material resources. This process does not meet routine online testing during rice harvesting. Therefore, a rapid nondestructive testing technology is urgently needed to assess the quality of riceclusters and conduct real-time online monitoring.

Hyperspectral imaging technologies (HSIs) have received considerable attention for food quality and safety(Pu et al.,2015, Cheng and Sun., 2015). In the evaluation of the quality of food, such as fruits (Keresztes, et al., 2016), vegetables(Liu et al., 2016), meat(Kamruzzaman, et al., 2016) and milk(Lim, et al., 2016), spectral analysis technology has been widely used as a fast and nondestructive tool for decades. However, the application of HSI on rice (with chaff) detection has been rarely reported in China. HSI which is an emerging nondestructive testing technology that combines traditional spectroscopy techniques with spectral and digital imaging, thereby providing not only the spectral information of the detected substance but also its space and spatial information(Li,

et al.,2017, El-Hajje, et al., 2016). HSI has been gradually applied to food quality and safety testing(Liu et al.,2017, Su and Sun, 2018, Pu et al.,2015). HSI can analyse the composition of rice on the basis of spectral techniques. The ultimate goal of this study is to develop an online monitoring instrument for rice protein content through the established PLSR (protein content) model and scanned HSI images.

II. Materials and Methods

2.1. Sample Preparation and Protein Content Determination

To study the rapid detection protein content of rice(with chaff), we selected 87 varieties of rice comprising 43 kinds of japonica-type rice, 30 kinds of indica-type rice and 14 kinds of glutinous rice. The rice samples were collected from research institutes and seed distributors in various regions of China. All samples of rice with healthy grain and uniform sizes were selected for ultrafine pulverisation to form a uniform powder. After drying, 0.5 g sample was weighed, and the heavy protein content of the sample was determined by Kjeldahl method (GB 5009.5-2016). Three parallel tests were performed. Each rice variety was scanned four times by a HSI system. Amongst the 87 rice samples, 58 and 29 rice samples were selected for calibration and model verification, respectively. Three classified rice protein content ranges are shown in Table 1, as follows:

Table 1 Actual measurement of protein content range in different rice varieties

Variety (With Chaff)	Protein Content (%)	
	Minimum	Maximum
Japonica-Type Rice	5.194	8.193
Indica-Type	5.618	8.850
Glutinous Rice	6.580	8.119

2.2. HSI System

A black box (IRCP0076-2COMB, Isuzu Optics Corp., Taiwan, China) included visible light and infrared switching mechanisms, a bottom plate, a support frame, a transmission light source, a diffuse light source mount and a light shield cover, an outer box and a stage(IRCP0076-1COMB, Isuzu Optics Corp., Taiwan, China), an infrared light source (IRCP0078-1COMB, Isuzu Optics Corp., Taiwan, China), a double-branched halogen light source (1000–2500 nm), 1000–2500 nm hyperspectral imager [N25E-SWIR,Specim,Finland], wavelength range: 1000–2500 nm; spectral resolution [with 30 μm slit]: 12 nm; lens [LES30, Specim, Finland], focal length: 30.7 mm, C-Mount, 900–2500 nm), an acquisition analysis software (IRCP0072-1COMB, Isuzu Optics Corp, Taiwan, China), a spectral image system software, an image processor (DELL, USA): 4G memory and a 1 T hard drive.

2.3. Image Acquisition and Correction

Rice is evenly filled in a culture dish (φ9 cm × 1 cm) which is compacted and placed directly beneath the mobile platform camera. Then, the same calibration whiteboard (*W*) was used for blank calibration to set the maximum emissivity (~99%), and the lens cap was covered for dark correction (*B*) to set the minimum reflectance (~0). Whilst using the software to control the platform movement, the culture dish was moved to the camera field of view, thereby adjusting the moving speed and exposure time to obtain a hyperspectral image. The original acquired image (I_0) was obtained.The calibration image (*I*) was calibrated by the HSIAnalyser spectral image processing software combined with W and B. A scanning image and a calculation picture are shown in Figure 1. The equation is as follows:

$$I = \frac{I_0 - B}{W - B}. \qquad (1)$$

2.4. Spectral Extraction

Using the spectral analysis software of Isuzu Optics Corp. instrument to select the scanned image of each sample, the spectral data of absorption intensity and wavelength can be automatically derived. The text files of the spectra were converted using the Origin charting software to obtain a curve image, with the horizontal axis as the wavelength and the vertical axis as the absorption intensity.

2.5. Chemometrics Analysis

The data extracted from the hyperspectral image is imported into the TQ Analyst software and processed by partial least squares regression (PLSR). PLSR is a reliable and effective method widely used in establishing mathematical models in food(Cheng and Sun,2017, Qiu and Wang, 2017, Su et al.,2017). PLSR can handle multicollinearity problems and allow variables higher than the samples, thereby that showing that it has a predictive function(Indahl et al.,2009).The software was used to establish calibration and verification models between the spectral data of different rice varieties. In this research, a quantitative calibration model between spectra has been created, and the protein content reference value has been analysed by PLSR.

2.6. Modelling Validation and Evaluation

An essential step in the model building process was model validation. Complete cross-validation can assess the accuracy and applicability of the model. A total of 29 rice variety samples were used for model validation. The accuracy of the model was verified by comparing the protein content (measured protein content in 29 rice varieties) with the model established by 58 rice varieties through chemical methods. The coefficients (calibration [R^2_C], cross-validation [R^2_{CV}] and prediction [R^2_P]) and error (root mean square calibration error [RMSEC], cross-validation [RMSECV] and prediction [RMSEP]) can have a critical impact on the model. In general, a qualitative model is determined by the following viewpoint: the higher the R^2_C, R^2_{CV} and R^2values are, the lower the RMSEC, RMSECV and RMSEP values will be(Zhu et al.,2016, Husnizar et al., 2018, Rohman et al.,2016).

2.7. Characteristic Wavelength Selection

The obtained hyperspectral image is characterised by multicolinearity between high-dimensional, continuous bands, thereby reducing the calculation speed of the calibration process and lowering the prediction model accuracy. Applying wavelength selection methods to HSI data in applications such as food quality evaluation, food safety and adulteration detection can considerably improve the prediction results(Liu et al.,2014, Hemmateenejad et al., 2007, Osborne et al.,1997). Therefore, selecting several characteristic wavelengths is necessary. In this study, the wavelengths corresponding to the regression coefficients are selected. Initially, the wavelengths with high regression coefficients are selected first, and the most representative wavelengths are selected to represent the full-band PLSR model. The model has been initially optimised using other wavelength combinations that are significantly representative. Comparing the results showed that the optimal combination was selected to determine the prediction model. In the process, the wavelength range was 1000–2500 nm (ElMasry et al., 2011). Figure 2 shows the key steps of the experiment by using the HSI technique.

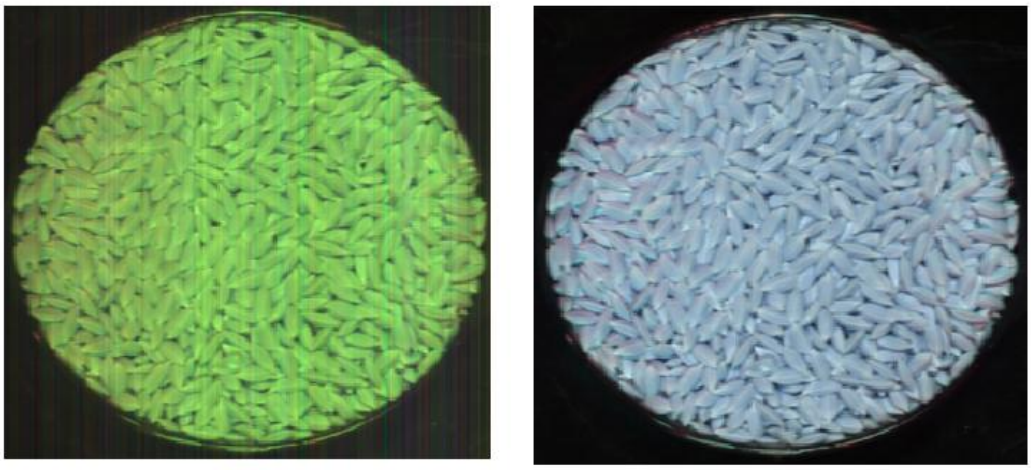

a. Unprocessed hyperspectral scan image b. Images processed by ref–white, ref–dark and sample data paths
Fig.1 Hyperspectral scan image of rice (with chaff)

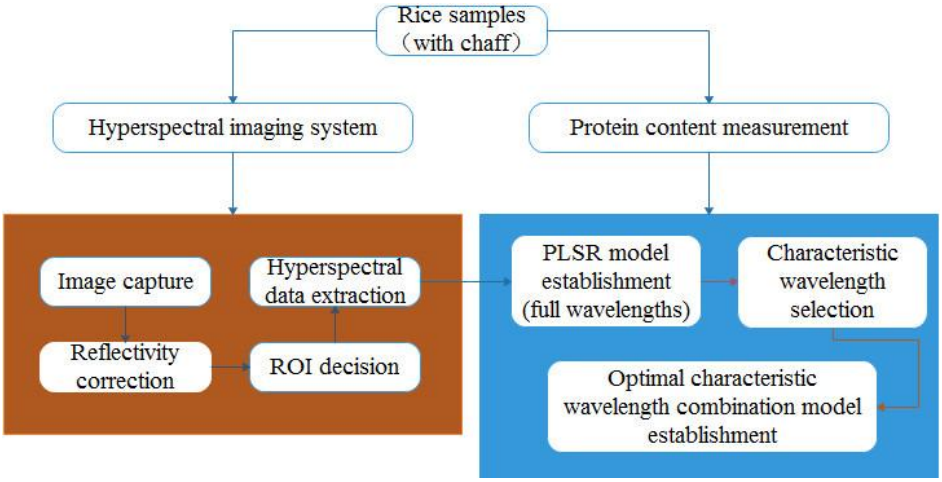

Fig.2 Key steps of experiment by using hyperspectral imaging technique

III. Results and Discussion

3.1. Spectral Features

Figure 3 shows the average reflectance spectra extracted from different rice varieties (with chaff). The wavelength range of 1000–2500nm is chosen as the research focus. The spectral wavelength is 1000–2500 nm, and the reflectivity is 0.3–0.9. The main absorption band is the combined absorption of O–H, C–H, N–H and C–O bonds and their strong overtone effect. In the wavelength range of 1000–2300 nm, the spectral reflectance develops in a similar trend. However, some significant differences amongst them are observed. These differences are attributed to the different quality attributes of different rice varieties. The uneven surface structure of the sample and the unfixed scattering of the sample surface also affect the spectral reflectance. The absorption peaks are mainly exhibited at 1173, 1404, 1697, 1898, 2036 and 2222 nm. The absorption peak in the 1690–1725nm band is formed by the first overtone of the C–H bond. The absorption peak at 1890–1925 nm is formed by H bonding in the O–H bond. The absorption peak at 2030–2065 nm is formed due to the stretching and bending combination of the O–H bond; the absorption peak at 2210–2245 nm is formed due to the extension of the C–O bond. After the wavelength is 2200 nm, the curve shows an irregular trendwhich is caused by the excessively large energy in the band scanning process and decrease in noise reduction effect(Jin, et al.,2015, Liu et al.,2014).

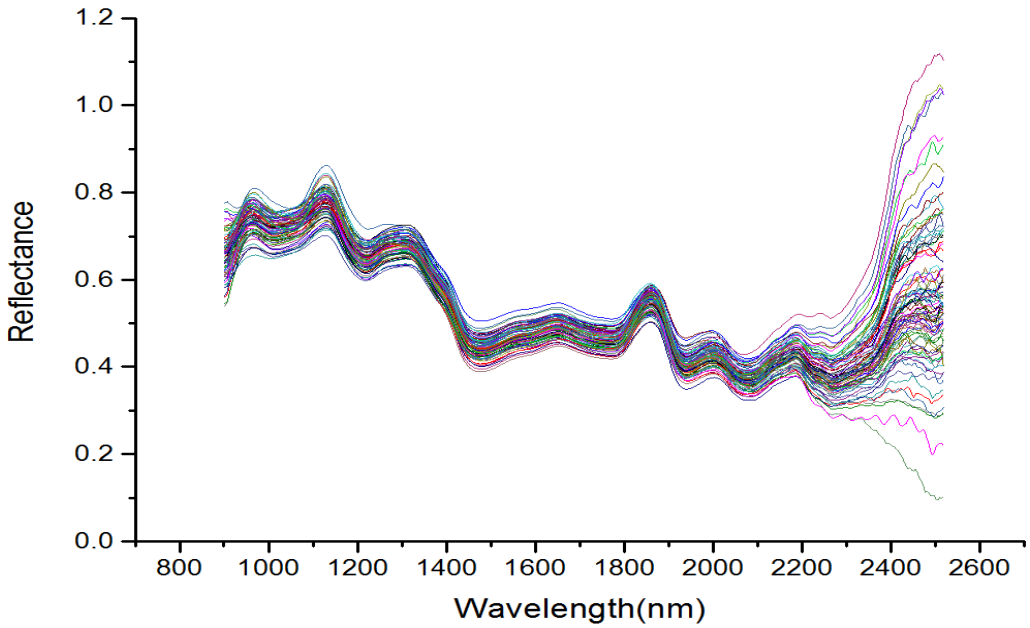

Fig.3 Average spectral data of the examined rice (with chaff) in 1000–2500 nm

3.2. Protein Content Calibration by Using Full Spectral Range

The correction, cross-validation and prediction models have been built using the PLSR on the basis on all spectral data extracted from the hyperspectral image and their corresponding measured protein content. As shown in Table 2, the calibration, cross-validation and prediction results of the models are evaluated by R^2_C, R^2_{CV} and R^2_P; the corresponding RMSEC, RMSECV and RMSEP, are used to identify the usefulness of the model. The R^2_C and R^2_{CV} values of the model are 0.992 and 0.993, and the RMSEC and RMSECV values of the model are 0.697% and 0.624%, respectively. The results show that the PLSR model performs well in both calibration and cross-validation. All calibration models have been built based on all 87 sample varieties. Figure 4, 5 and 6 illustrate the regression analysis diagrams of the correction, the cross-validation and prediction models, respectively. 'Corr. Coeff' represents the correction factor. As shown in Table 2, the $R^2_P$and RMSEP values of the model are 0.970 and 1.03%, respectively. The results suggest a stable predictive accuracy for rice protein content. The model has been validated with accurate coefficient of determination (R^2_C, R^2_{CV} and R^2_P) and minimal root mean square error (RMSEC, RMSECV and RMSEP). Overall, the established PLSR model has accurate predictive power and robust stability, and HSI can be used as a nonbreaking technique to detect the rice protein content.

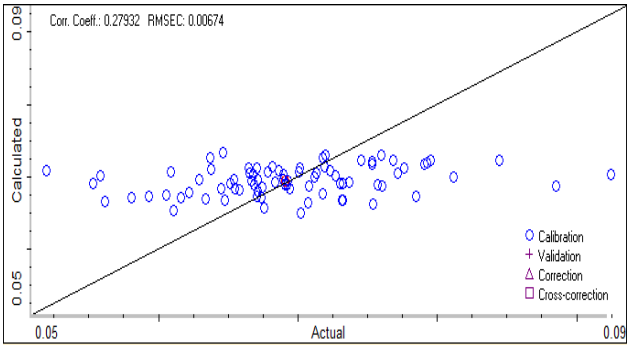

Fig.4 Calibration model scatter plot

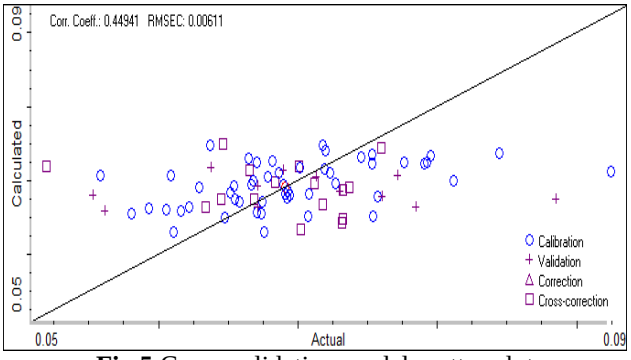

Fig.5 Cross-validation model scatter plot

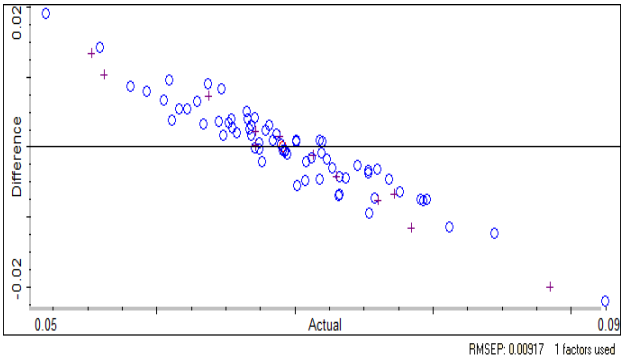

Fig.6 Prediction model scatter plot

Table 2 Calibration and prediction results of rice protein content by using full spectral range

Protein model	Spectral range(nm)	No. of varieties	Calibration		Cross-validation		Prediction	
			R^2	RMSEC(%)	R^2_{CV}	RMSECV(%)	R^2_P	RMSECP(%)
PLSR	1000-2500	87	0.992	0.697	0.993	0.624	0.970	1.03

3.3. Protein Content Modelling via PLSR by Using Selected Optimal Wavelengths

The optimal wavelength is significant andIt provides effective information to predict the rice protein value which minimises the amount of information and scan time needed. In this study, characteristic wavelengths have been chosen based on the regression coefficients of the established PLSR model. The model has been established by selecting the combination of wavelengths, with the largest regression coefficient values from all wavelengths with characteristic peaks (regardless of the sign). Seven independent wavelengths (i.e. 1005, 1173, 1404, 1697, 1898, 2036 and 2222 nm) are selected to initially for the model. The shape and size of the absorption peaks in the near-infrared spectral region are affected by the vibration of different components of the functional group. For example, water, protein and fat are associated with the combined vibration and overtone of the C–H, O–H and N–H bonds. Another seven wavelengths are selected to form different combinations to establish a PLSR model. The coefficients and errors of correction and cross-validation are shown in Table 3. The optimal wavelength combination is selected by R^2_c,RMSEC, R^2_{cv} and RMSECVvalues. The higher the R^2 and R^2_{cv}values

are, the better the model fit will be. The smaller the RMSEC and RMSECVvalues are, the greater of the model accuracy will be. In combination with the description above, the wavelengths of the four values (i.e., 1005, 1404, 2036 and 2222 nm) are determined as the optimum wavelength combination. Therefore, the model should be simplified using the two sets of determined optimal wavelength combinations. The model whose stability and accuracy are evaluated by determining the coefficient and root mean square error is redesigned. According to the full spectrum modelling method, the determined optimal wavelength range is selected; the four wavelengths include 1005, 1404, 2036 and 2222 nm. The optimal feature wavelength combination that can reduce costs and increase the efficiency when it is applied to actual production is selected.

Table 3 Coefficient and error of different combinations of characteristic wavelengths

Important wavelengths (nm)	Calibration		Cross-validation	
	R^2	RMSEC (%)	R^2_{CV}	RMSECV (%)
1005,1173,1404,1697,1898,2036,2222	0.997	0.680	0.993	0.635
1005,1173,1404,1697,2036,2222	0.998	0.679	0.997	0.637
1005,1404,1697,1898,2036,2222	0.996	0.684	0.996	0.643
1005,1173,1404,1697,2222	0.996	0.679	0.996	0.628
1005,1173,1697,1898,2222	0.998	0.685	0.997	0.640
1005,1404,2036,2222	0.999	0.684	0.999	0.625
1005,1898,2222	0.997	0.690	0.997	0.646

IV. Conclusions

HSI is feasible in predicting the rice sample protein content in the wavelength range of 1000–2500 nm. The full-spectrum prediction model, that is, PLSR, has an extremely high R^2 value (0.992). Cross-validation (R^2_{CV}= 0.993) and prediction models (R^2_P = 0.970) also have high correlation coefficients, thereby indicating that the model performs well. A simplified regression model has been established using four optimal characteristic wavelengths, and the regression coefficients have been optimised. The characteristic wavelength model is built to save time in scanning spectra compared with the full-wavelength model, whilst the model accuracy and stability are improved. The study sample covers 87 different ricevarieties (with chaff) in China. HSI as a nondestructive testing technology can be potentially applied by the spectrum in the future.

Acknowledgement

This research was funded by the National Natural Science Foundation of China (grant no. 31471676) and Higher Education Superior Discipline Team Training Program of Shandong Province. The author would like to thank CaiHongzhen and Wang Fang for their help.

References

[1]. Maraseni, Tek Narayan, et al. "An international comparison of rice consumption behaviours and greenhouse gas emissions from rice production." *Journal of Cleaner Production* 172 (2018): 2288-2300. https://doi.org/10.1016/j.jclepro.2017.11.182

[2]. Sompong, R., et al. "Physicochemical and antioxidative properties of red and black rice varieties from Thailand, China and Sri Lanka." *Food chemistry* 124.1 (2011): 132-140. https://doi.org/10.1016/j.foodchem.2010.05.115

[3]. Lin, Kai, et al. "The arsenic contamination of rice in Guangdong Province, the most economically dynamic provinces of China: arsenic speciation and its potential health risk." *Environmental geochemistry and health* 37.2 (2015): 353-361. DOI 10.1007/s10653-014-9652-1

[4]. Naito, Shigehiro, et al. "Effects of polishing, cooking, and storing on total arsenic and arsenic species concentrations in rice cultivated in Japan." *Food chemistry* 168 (2015): 294-301. https://doi.org/10.1016/j.foodchem.2014.07.060

[5]. Wattanasiritham, Ladda, et al. "Isolation and identification of antioxidant peptides from enzymatically hydrolyzed rice bran protein." *Food chemistry* 192 (2016): 156-162. https://doi.org/10.1016/j.foodchem.2015.06.057

[6]. Kamruzzaman, Mohammed, et al. "Assessment of visible near-infrared hyperspectral imaging as a tool for detection of horsemeat adulteration in minced beef." *Food and bioprocess technology* 8.5 (2015): 1054-1062. DOI 10.1007/s11947-015-1470-7

[7]. Jackson, Peter E., et al. "Determination of total nitrogen in food, environmental and other samples by ion chromatography after Kjeldahl digestion." *Journal of Chromatography A* 546 (1991): 405-410. https://doi.org/10.1016/S0021-9673(01)93039-0

[8]. Zhang, Chu, et al. "Application of near-infrared hyperspectral imaging with variable selection methods to determine and visualize caffeine content of coffee beans." *Food and bioprocess technology* 10.1 (2017): 213-221. DOI 10.1007/s11947-016-1809-8

[9]. Pu, Hongbin, et al. "Classification of fresh and frozen-thawed pork muscles using visible and near infrared hyperspectral imaging and textural analysis." *Meat Science* 99 (2015): 81-88. https://doi.org/10.1016/j.meatsci.2014.09.001.

[10]. Cheng, Jun-Hu, and Da-Wen Sun. "Rapid and non-invasive detection of fish microbial spoilage by visible and near infrared hyperspectral imaging and multivariate analysis." *LWT-Food Science and Technology* 62.2 (2015): 1060-1068. https://doi.org/10.1016/j.lwt.2015.01.021

[11]. Keresztes, Janos C., Mohammad Goodarzi, and Wouter Saeys. "Real-time pixel based early apple bruise detection using short wave infrared hyperspectral imaging in combination with calibration and glare correction techniques." *Food Control* 66 (2016): 215-226. https://doi.org/10.1016/j.foodcont.2016.02.007

[12]. Liu, Changhong, et al. "Potential of multispectral imaging for real-time determination of colour change and moisture distribution in carrot slices during hot air dehydration." *Food chemistry* 195 (2016): 110-116. https://doi.org/10.1016/j.foodchem.2015.04.145

[13]. Kamruzzaman, Mohammed, Yoshio Makino, and Seiichi Oshita. "Rapid and non-destructive detection of chicken adulteration in minced beef using visible near-infrared hyperspectral imaging and machine learning." *Journal of Food Engineering* 170 (2016): 8-15. https://doi.org/10.1016/j.jfoodeng.2015.08.023

[14]. Lim, Jongguk, et al. "Detection of melamine in milk powders using near-infrared hyperspectral imaging combined with regression coefficient of partial least square regression model." *Talanta* 151 (2016): 183-191.
[15]. https://doi.org/10.1016/j.talanta.2016.01.035
[16]. Xie, Li, et al. "Hyperspectral image classification using discrete space model and support vector machines." *IEEE Geoscience and Remote Sensing Letters* 14.3 (2017): 374-378.https://doi.org/10.1109/LGRS.2016.2643686
[17]. El-Hajje, Gilbert, et al. "Quantification of spatial inhomogeneity in perovskite solar cells by hyperspectral luminescence imaging." *Energy & Environmental Science* 9.7 (2016): 2286-2294. https://doi.org/10.1039/C6EE00462H
[18]. Liu, Yuwei, Hongbin Pu, and Da-Wen Sun. "Hyperspectral imaging technique for evaluating food quality and safety during various processes: A review of recent applications." *Trends in Food Science & Technology* 69 (2017): 25-35. https://doi.org/10.1016/j.tifs.2017.08.013
[19]. Su, Wen-Hao, and Da-Wen Sun. "Fourier transform infrared and Raman and hyperspectral imaging techniques for quality determinations of powdery foods: a review." *Comprehensive Reviews in Food Science and Food Safety* 17.1 (2018): 104-122. https://doi.org/10.1111/1541-4337.12314
[20]. Pu, Yuan-Yuan, Yao-Ze Feng, and Da-Wen Sun. "Recent progress of hyperspectral imaging on quality and safety inspection of fruits and vegetables: a review." *Comprehensive Reviews in Food Science and Food Safety* 14.2 (2015): 176-188. https://doi.org/10.1111/1541-4337.12123
[21]. Cheng, Jun-Hu, and Da-Wen Sun. "Partial least squares regression (PLSR) applied to NIR and HSI spectral data modeling to predict chemical properties of fish muscle." *Food Engineering Reviews* 9.1 (2017): 36-49. DOI 10.1007/s12393-016-9147-1
[22]. Qiu, Shanshan, and Jun Wang. "The prediction of food additives in the fruit juice based on electronic nose with chemometrics." *Food chemistry* 230 (2017): 208-214.
[23]. https://doi.org/10.1016/j.foodchem.2017.03.011
[24]. Su, Wen-Hao, Hong-Ju He, and Da-Wen Sun. "Non-destructive and rapid evaluation of staple foods quality by using spectroscopic techniques: a review." *Critical reviews in food science and nutrition* 57.5 (2017): 1039-1051. https://doi.org/10.1080/10408398.2015.1082966
[25]. Indahl, Ulf G., Kristian Hovde Liland, and Tormod Næs. "Canonical partial least squares—a unified PLS approach to classification and regression problems." *Journal of Chemometrics: A Journal of the Chemometrics Society* 23.9 (2009): 495-504. https://doi.org/10.1002/cem.1243
[26]. Zhu, Yun, Guangrong Shen, and Qiaoqiao Xiang. "Quantitative analysis of salinized soil reflectance spectra during microbial remediation processes based on PLSR." *2016 Fifth International Conference on Agro-Geoinformatics (Agro-Geoinformatics)*. IEEE, 2016.
[27]. https://doi.org/10.1109/Agro-Geoinformatics.2016.7577608
[28]. Husnizar, H., Wahyu Wilopo, and Ahmad Tawfiequrrahman Yuliansyah. "The prediction of heavy metals lead (Pb) and zinc (Zn) contents in soil using NIRs technology and PLSR regression method." *Journal of Degraded and Mining Lands Management* 5.3 (2018): 1153. DOI:10.15243/jdmlm.2018.053.1153
[29]. Rohman, Abdul, et al. "Fourier transform infrared spectroscopy combined with multivariate calibrations for the authentication of avocado oil." *International journal of food properties* 19.3 (2016): 680-687. https://doi.org/10.1080/10942912.2015.1039029
[30]. Liu, Dan, Da-Wen Sun, and Xin-An Zeng. "Recent advances in wavelength selection techniques for hyperspectral image processing in the food industry." *Food and Bioprocess Technology* 7.2 (2014): 307-323. DOI 10.1007/s11947-013-1193-6
[31]. Hemmateenejad, Bahram, Morteza Akhond, and Fayezeh Samari. "A comparative study between PCR and PLS in simultaneous spectrophotometric determination of diphenylamine, aniline, and phenol: effect of wavelength selection." *Spectrochimica Acta Part A: Molecular and Biomolecular Spectroscopy* 67.3-4 (2007): 958-965. https://doi.org/10.1016/j.saa.2006.09.014
[32]. Osborne, ScottáD, and RobertáB Jordan. "Method of wavelength selection for partial least squares." *Analyst* 122.12 (1997): 1531-1537. https://doi.org/10.1039/A703235H
[33]. ElMasry, Gamal, Da-Wen Sun, and Paul Allen. "Near-infrared hyperspectral imaging for predicting colour, pH and tenderness of fresh beef." *Journal of Food Engineering* 110.1 (2012): 127-140. https://doi.org/10.1016/j.jfoodeng.2011.11.028
[34]. Jin, Huali, Linlin Li, and Junhu Cheng. "Rapid and non-destructive determination of moisture content of peanut kernels using hyperspectral imaging technique." *Food analytical methods* 8.10 (2015): 2524-2532. DOI 10.1007/s12161-015-0147-1
[35]. Liu, Dan, Da-Wen Sun, and Xin-An Zeng. "Recent advances in wavelength selection techniques for hyperspectral image processing in the food industry." *Food and Bioprocess Technology* 7.2 (2014): 307-323. DOI 10.1007/s11947-013-1193-6

Figure Captions/Figure Legends

Fig.1 Plot of hyperspectral scan image of rice (with chaff).A unprocessed; B processed by ref–white, ref–dark and sample data paths.
Fig.2 Plot of key steps of experiment by using hyperspectral imaging technique.
Fig.3 Plot of average spectral data of the examined rice (with chaff) in 1000-2500 nm.
Fig.4 Plot of calibration model scatter plot.
Fig.5 Plot of cross-validation model scatter plot.
Fig.6 Plot of prediction model scatter plot.

Zhehao Zhang. " Nondestructive Determination of Rice (with Chaff) Protein Content by Using Hyperspectral Imaging Technique." IOSR Journal of Environmental Science, Toxicology and Food Technology (IOSR-JESTFT) 13.9 (2019): 11-17.